ECRONICON OPEN ACCESS

EC PROTEOMICS AND BIOINFORMATICS
Research Article

Protein Concentration and Relaxation Properties Inferred from Quantified Quadrupole Peaks Measured by Relaxometry

Abdul Nashirudeen Mumuni*

Department of Medical Imaging, School of Allied Health Sciences, University for Development Studies, Tamale, Ghana

***Corresponding Author:** Abdul Nashirudeen Mumuni, Department of Medical Imaging, School of Allied Health Sciences, University for Development Studies, Tamale, Ghana.
E-mail: mnashiru@uds.edu.gh

Received: April 01, 2024; **Published:** May 15, 2024

Abstract

Relaxometry is a nuclear magnetic resonance technique that can non-invasively measure the concentration of proteins in tissue at varying magnetic field strengths and constant temperature, inferred from cross-relaxation processes of protein protons in water. These cross-relaxation processes are associated with quadrupole dips that can be measured at established frequencies to infer protein content. In the absence of standardized quantification methods of the size of the quadrupole dips, this study suggested the basic striped trapezium mathematical method of estimating the total area of quadrupole peaks measured from *in vitro* protein-mimicking samples made from varying concentrations of bovine serum albumen dissolved in phosphate buffer saline. The quantification method was implemented on an inverse of the quadrupole dip, resulting in a quadrupole peak, which was extracted from total relaxation processes including background relaxation. The quadrupole peaks were striped into smaller trapezia, the area of each of which was calculated using the formula for calculating the area of a trapezium. An algebraic sum of these striped trapezia yielded the total quadrupole peak area recorded from each protein sample. Consistent with theoretical predictions, the area of each quadruple peak was proportional to its protein content and relaxivity. It was also found that while agarose, a relaxation-modifying agent, prolonged the T_1 relaxation time of the samples thus reducing the size of the quadruple peaks, $CuSo_4$, a contrast agent, shortened the T_1 relaxation times without changing the size of the quadrupole peak. The relaxometry results compared with field-cycling magnetic resonance imaging results for samples without contrast, but those with contrast showed remarkedly different results between the two methods. The study therefore confirms theoretical underpinnings of relaxometry as a tool for interrogating protein concentration changes in samples.

Keywords: *Fast Field Cycling; Relaxometry; Spin-Lattice Relaxation; Quadrupole Peak; Bovine Serum Albumen; Magnetic Resonance Imaging*

Abbreviations

BSA: Bovine Serum Albumin; FFC: Fast Field Cycling; IR: Inversion Recovery; MHz: Mega-Hertz; MR: Magnetic Resonance; MRI: Magnetic Resonance Imaging; NMR: Nuclear Magnetic Resonance; NQR: Nuclear Quadrupole Resonance; PBS: Phosphate Buffer Saline; R_1: Spin-Lattice Relaxation Rate; RF: Radiofrequency; T_1: Spin-Lattice Relaxation Time

Introduction

Nuclear magnetic resonance (NMR) relaxometry measures protein concentrations *in vivo*. It provides information about tissue integrity in early stages of protein-related diseases such as Alzheimer's and cancer [1,2]. The technique involves the measurement of T_1 relaxation rates of a specimen as a function of magnetic field strength, B_0 varied rapidly over a given range during the pulse sequence, a process known as fast field cycling (FFC). In FFC, the B_0 field switching time is less than the T_1 relaxation time of the sample. T_1 is particularly suitable in relaxometry studies because T_1 in tissues is strongly dependent on field strength (gets longer with increasing field strength) while T_2 is hardly influenced by changes in field strength [3].

While operational magnetic resonance imaging systems with variable field strength are yet to be introduced into routine research and clinical applications, laboratory-based FFC systems are currently being used to study the molecular dynamics and relaxation properties of samples, *in vitro*. Dispersion curves, consisting of quadrupole peaks, generated from the field-cycling relaxometer are often evaluated qualitatively or quantitatively through area-under-curve methods to infer protein concentrations [2,4].

Relaxometry is based on the nuclear quadrupole resonance (NQR) phenomenon. In NQR, the energies of nuclei with an electric quadrupole moment are split by an electric field gradient that has been created by the electronic bonds in the local environment. The nuclei are then set in a static inhomogeneous electric field, allowing the absorption of energy from a radiofrequency field. Any nucleus with more than one unpaired nuclear particle (the nuclear particles being protons or neutrons) will have a quadrupolar charge distribution. Examples of such nuclei are nitrogen-14 (^{14}N), chlorine-35 (^{35}Cl) and copper-63 (^{63}Cu). The resonance interaction of this quadrupole with an electric field gradient supplied by the non-uniform distribution of electron density (from bonding electrons) results in the NQR effect. NQR is therefore very sensitive to the kind of bonds surrounding the quadrupolar nucleus [3].

The approximate Larmor frequency range for NQR experiments are within 1 to 1000 MHz range [4]. This study used a range of 1.5 to 3.5 MHz to observe the NQR effect in protein samples. The protein samples have ^{14}N-^{1}H groups [5] that serve as "relaxation sinks" in order to enhance proton relaxation due to their interactions with the ^{14}N quadrupolar nucleus [2,4]. This causes reductions in the proton spin-lattice relaxation time, T_1, called "quadrupole dips" (where $1/T_1$ is called a "quadrupole peak"), which occur at three frequencies corresponding to the ^{14}N nuclear quadrupole transitions. The transition frequencies are observed at field strengths of 65 mT, 49 mT and 16 mT (or 2.8 MHz, 2.1 MHz and 0.7 MHz, respectively, for the proton Larmor frequencies) [2-4,6]. It has been suggested that the size of the quadrupole peak may provide a noninvasive measure of immobilized protein content in most tissues [1].

In the absence of a standardized quantitative method for interrogating protein concentrations of samples in relaxometry, there is a need to develop an in-house method which is simple, accurate and reproducible under several experimental conditions.

Objectives of the Study

The objectives of this study were therefore to develop a quantitative method of estimating the size of quadrupole peaks from relaxometry experiments on protein-based phantoms, evaluate the sensitivity (to protein concentration changes) of the FC relaxometer for the study, assess the effect of contrast and relaxation-modifying agents on relaxation dynamics of protein, and validate the relaxometry results with low-field FC magnetic resonance imaging of the protein phantoms.

Materials and Methods

Preparation of protein phantoms

Bovine serum albumen (BSA) was the main protein aggregate for the study, mixed with either one or two of the following agents (Figure 1): agarose, phosphate buffer saline (PBS) and copper sulphate ($CuSO_4$). While BSA and agarose were dried powders, PBS was diluted in 1:3 parts of deionized water. Different $CuSO_4$ solutions of the required molarities were prepared by dissolving a weighed mass of $CuSO_4$ crystals in 1 liter of deionized water.

Figure 1: *From left to right; a volumetric flask of $CuSO_4$ solution, BSA (in white container), PBS, composite protein phantom, and NMR tube containing BSA gel (in front of PBS).*

Three different types of BSA gels were prepared: 'BSA in PBS', 'BSA and agarose in PBS' and 'BSA in $CuSO_4$ solution'. The use of PBS was because it easily dissolves BSA and also provides similar conditions to proteins in human tissues. All samples were prepared in glassware thoroughly washed with a powerful decontaminant, rinsed with deionized water and air-dried.

Preparation of BSA in PBS

The required percentage by weight of BSA was weighed (in grams) on an electronic balance and carefully transferred into a small beaker of 5 cm^3 of dilute PBS. The BSA-PBS mixture was gently warmed in a water bath at a temperature of 40°C while stirring with a spatula. The temperature was slowly raised to 80°C, while stirring continued. This continued for approximately 10 minutes to achieve complete dissolution of the BSA in the PBS. 1 ml of the resulting solution was syringed into an NMR tube, which was further heated (with a smaller beaker covering its open end to prevent significant vapor loss from the contents) in the water bath. The temperature was raised to 95°C and heating continued for 30 minutes. During this period, the BSA-PBS mixture had changed to gel.

Preparation of BSA and agarose in PBS

The required percentages by weight of BSA and agarose were weighed (in grams) on an electronic balance, separately, and transferred gently into a beaker of 5 cm^3 of PBS. The BSA-agarose-PBS mixture was then gently warmed, while stirring with a spatula, in a water bath at 40°C. The temperature was slowly increased to 95°C while stirring continued. A total heating time of 10 minutes, approximately, was allowed for a complete mixture to be attained. 1 ml of the resulting solution was syringed into an NMR tube which was heated (with the open end covered with a smaller beaker) at 95°C continuously for 35 minutes, during which period the contents have transformed into gel.

Preparation of BSA in $CuSO_4$ solution

The required percentages by weight of BSA were added to 5 cm^3 of $CuSO_4$ solution in a small beaker and gently warmed, while stirring with a spatula, in a water bath at 40°C. The temperature was slowly raised to 80°C. An approximate period of 10 minutes was allowed to attain a uniform mixture. 1 ml of the resulting solution was syringed into an NMR tube which was then further heated (with a smaller beaker covering the open end) in the water bath at 90°C for 30 minutes. During this period, the contents of the tube had changed to a gel.

Sample handling

After the gel had been formed in each preparation, the sample tube was removed from the water bath, wiped dry with a tissue paper, covered with a tight-fitting cork at the open end and labelled by content's name and preparation date. This labelled tube was then refrigerated overnight.

Before an experiment with a sample (from the fridge), it was warmed for a period of 10 minutes at room temperature (25°C) before placement in the relaxometer; then left for another waiting period of 10 minutes to ensure complete equilibration of its temperature just before data acquisition.

The sample volume of 1 ml was crucial so that the sample did not extend beyond the homogeneous bounds of the RF coil in order for it to experience a homogeneous magnetic field. The necessity for a homogeneous field also required that the sample remained fixed, without movement of any sort, within the relaxometer (Figure 2) throughout the time scale of the experiment.

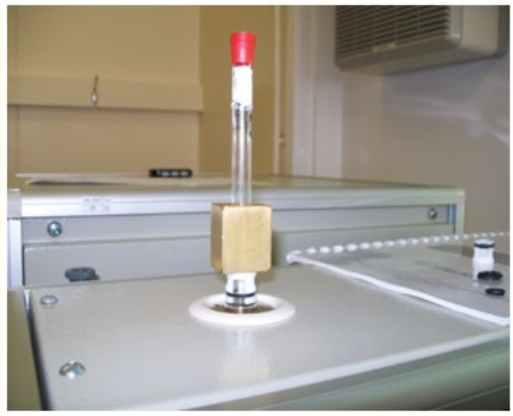

Figure 2: *Sample positioning during data acquisition in the relaxometer. The clamp and load provide a firm grip and stable position of the sample tube against expulsion by the air pressure around it.*

A composite phantom was made by holding firmly together with a sellotape seven NMR tubes containing the different preparations (Figure 3). This phantom was imaged using a low-field FC MRI scanner (Figure 6).

Figure 3: *The composite phantom, made up of seven NMR tubes of different sample concentrations.*

Field cycling relaxometry

Relaxometry data was acquired using a Stelar SMARtracer FFC relaxometer (Figure 4) equipped with a multifunctional NMR console for carrying out NMR measurements [7]. The console of the relaxometer consists of four parts: a computer, RF power transmitters/ receiver, temperature/flow-rate control unit and the main magnet.

Figure 4: *"Stelar SMARtracer FFC relaxometer" and accessories.*

The pulse sequence timing and parameter settings of all measurements are controlled by a powerful NMR software package installed on a Pentium M, 1.6 GHz, 512 MB ram, HD 60 GB single board computer with 4 USB and Ethernet ports. A high-resolution LCD monitor is connected to the computer for a visual output of all measurements.

The inversion recovery, IR pulse sequence (Figure 5) was selected as the sequence of choice for the experiments as it was found to show least errors in the relaxation measurements, consistency and robustness to RF pulse fluctuations (due to temperature drifts for example) in comparison to the other pulse sequences (at the same temperature) available on the relaxometer.

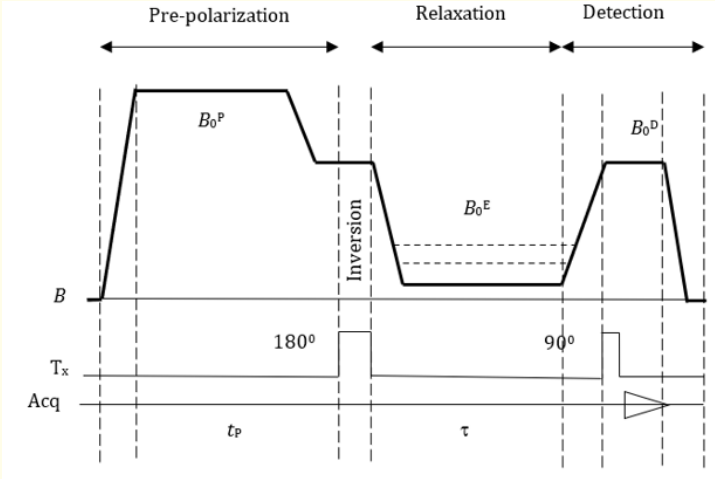

Figure 5: *The inversion recovery (IR) pulse sequence for the relaxometry measurements.*

The IR sequence (Figure 5) involves pre-polarizing the sample in the B_0^P field, then switching to B_0^D where the first 180° RF pulse is applied to invert the pre-polarized magnetization. The magnet is then switched to B_0^E where the sample is allowed to relax for a variable period τ. The field is then switched to a final B_0^D field where a 90° RF pulse is applied to generate the FID [8].

Field cycling magnetic resonance imaging

The composite phantom was imaged in a home-built, whole-body sized MR scanner (Figure 6) which operates on field compensation method of field-cycling: B_0^D field generated by the subtraction of variable field strengths from a fixed field by the use of two coaxial magnets [9].

Figure 6: *The Field Cycling MRI system used for the study.*

The outer, primary magnet (constructed from ferrite) generates a fixed, vertically oriented B_0^D field of 59 mT. This is a whole-body sized permanent magnet with an approximate mass of 2600 kg and a clear bore of 65 cm. Gradient coils are constructed into this magnet.

The inner, secondary magnet (made from sheets of copper conductor), when energized, generates an antiparallel variable magnetic field to the primary magnet's field; thus, reducing the net field at the sample. It is a resistive saddle-shaped coil with an outer diameter of 64 cm and is well-fitted into the primary magnet, creating a free bore diameter of 52 cm.

The whole support structure of the magnet and the ferrite are non-conducting and so there is no necessity for eddy current compensation during field cycling. The experimental laboratory is equipped with an air-conditioning unit to maintain a room temperature of 22 ± 0.5°C as the ferrite magnet has a relatively large temperature coefficient (-0.2% $°C^{-1}$). The temperature within the ferrite magnet structure itself is stabilized by a continuously operating fan that circulates air around it. The inner coil is also water cooled on its outer surface, and a network of platinum resistance thermometers is coupled to it for monitoring its temperature during operation.

The MR scanner is operated by a software on an IBM-compatible computer. Gradient and field cycling waveforms are generated from the computer console through four programmable 12-bit digital-to-analogue converters. The IR pulse sequence (Figure 5) was again used to image the phantom. In its implementation, an initial 10 ms adiabatic fast passage was used to provide a uniform inverted magnetization. The field was then switched to an evolution value of 59 mT for 30 ms and then returned to a detection field of 59 mT where the signal was read out, after a 70 ms delay, by a 90° pulse.

Quantification of the quadrupole peaks

The background T_1 relaxation processes in proteins can be described by a power law [4,10]:

$T_1 \alpha \upsilon_L^b$ [Equation 1]

which is expressed as a rate:

$R_1 \alpha \upsilon_L^{-b}$; (where $R_1 = 1/T_1$) [Equation 2]

where 'b' is usually in the range of 0.65 to 0.85 at room temperature and decays to lower values upon temperature reduction [4]; υ_L is the Larmor frequency of the acquisition.

For a complete description of the relaxation process referring to protons bound to protein backbones, two rate contributions are considered [11]:

$1/T_1 = R_1 = R_p + R_q$ [Equation 3]

where R_p refers to homonuclear dipolar coupling between protons (i.e. proton-proton interaction) and R_q refers to heteronuclear dipolar interaction between protons and non-resonant nuclei (i.e. the quadrupole peaks). R_p and R_q describe background and quadrupole relaxation processes, respectively.

Background relaxation rates, R_p over a range of 0.5 to 6.5 MHz were recorded and the resulting dispersion profiles were curve-fitted using Microsoft Excel (Figure 7) to generate an exponential equation of the form:

$R_p = k\upsilon_L^{-b}$ [Equation 4]

Relaxivities at 0.5 MHz, 2.1 MHz and 2.8 MHz were not included in these plots (Figure 7). The reasons were to avoid the significant error to be imposed on the measurement at 0.5 MHz by the sequence in use and to also exclude the quadrupole peaks (which occur at 2.1 MHz and 2.8 MHz) from the background plots.

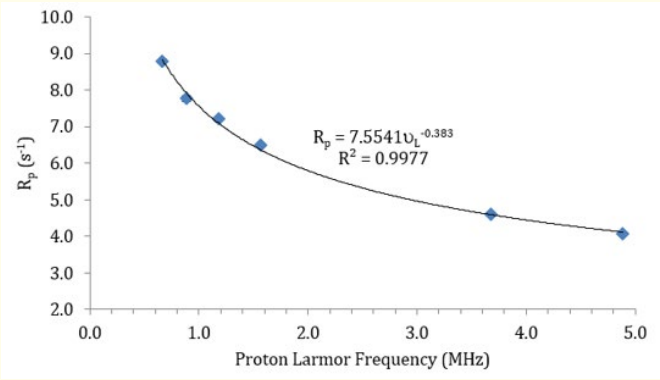

Figure 7: *Background relaxation curve of a 20% BSA sample. The R^2 value expresses the accuracy or 'goodness of the fit'.*

Relaxation rates were measured again over a narrower range (1.5 to 3.5 MHz), with particular consideration for inclusion of the quadrupole peaks (Figure 8).

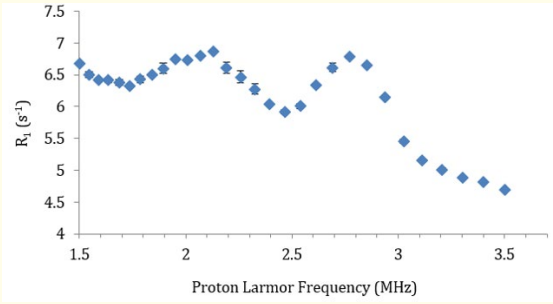

Figure 8: *R_1 dispersion profile of the 20% BSA sample showing the quadrupole peaks at 2.1 MHz and 2.8 MHz Larmor frequencies, resulting from the molecular interaction of water protons with protein protons of the immobilized peptide (^1H-^{14}N) bonds in the protein molecule; $R_1 = R_p^{/} + R_q$.*

The Larmor frequencies (υ_L) of Figure 8 were substituted into the equation of the curve-fit (Figure 7) to generate another set of relaxation rates, $R_p^{/}$ - these were the relaxations due to the background processes that added to the quadrupole processes (R_q) to yield the R_1 dispersion of Figure 8. Subtraction of $R_p^{/}$ from R_1 yielded the values of $\triangle R_1$ (or R_q), which were then plotted against the υ_L values of the quadrupole peak data set (Figure 9).

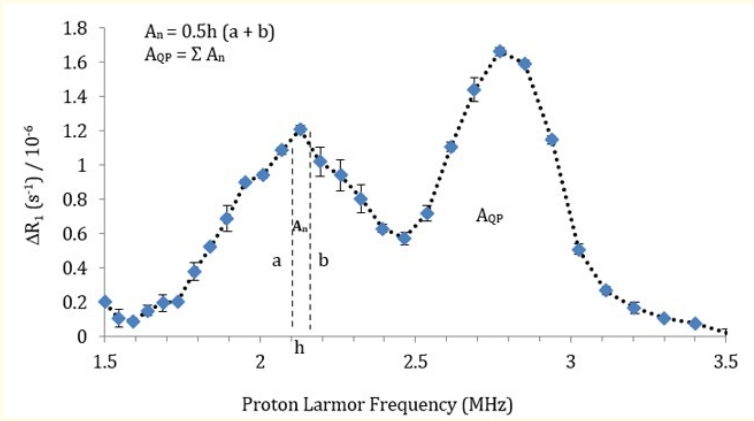

Figure 9: *The quadrupole peaks generated by plotting the relaxation difference ($\triangle R_1$) versus the Larmor frequencies of the quadrupole peak data set. The $\triangle R_1$ axis has been normalized to 10^{-6} to cancel out the 'mega' (10^6) unit of the Larmor frequencies so that the areas are in units of per squared second (s^{-2}).*

The sizes of the quadrupole peaks were then obtained by 'striping' them into smaller trapezia (with thickness defined by the frequency axis), calculating the area of each trapezium and summing the areas up. In order to enhance the accuracy of the computation, the lower tails of the peaks were ignored; thus, υ_L ranges of 1.8 to 2.5 MHz and 2.5 to 3.0 MHz were chosen for the peaks at 2.1 MHz and 2.8 MHz respectively.

Results and Discussion

The results are presented according to the objectives of the study, in sections presenting findings on quantification of the quadrupole peaks, sensitivity of the relaxometer, effects of agarose and $CuSO_4$ on relaxivity of protein, and comparison of the relaxometry and MRI results.

Protein concentration and relaxation dynamics inferred from quadrupole peak areas

Figure 10 shows a plot of five BSA samples whose concentrations were measured by relaxometry. The sizes of the peaks, by qualitative inspection, clearly show an increasing trend with increasing BSA concentration.

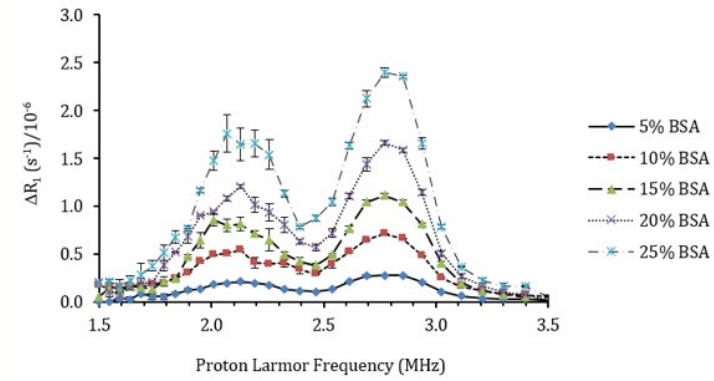

Figure 10: *Quadrupole peaks of five BSA concentrations.*

By applying the striped trapezium method of quantifying the area under, for example, the 20% BSA peak over a range of 1.8 to 2.5 MHz for the first peak and a range of 2.5 to 3.0 MHz for the second peak, Table 1 shows the striped trapezium areas of the two peaks. The sum of the stripes of each peak then yielded the peak sizes; the total protein concentration was then inferred from the total area of the two peaks as shown in Table 1.

Table 1: *Striped trapezia and total areas of the two quadrupole peaks recorded from the 20% BSA sample.*

First peak: (1.840 - 2.465) MHz				
$\_B_0^E\_\_\_\_$	$\triangle R_1/10^{-6}$	a+b	h	0.5*h(a+b)
2.4652	0.571751	1.203446	0.0712	0.042843
2.394	0.631695	1.434973	0.0689	0.049435
2.3251	0.803278	1.741218	0.0666	0.057983
2.2585	0.93794	1.95534	0.0657	0.064233
2.1928	1.0174	2.225772	0.0635	0.070668
2.1293	1.208372	2.290714	0.0602	0.068951
2.0691	1.082342	2.024748	0.0606	0.06135

2.0085	0.942406	1.845343	0.0573	0.052869
1.9512	0.902938	1.592524	0.0565	0.044989
1.8947	0.689587	1.212902	0.0546	0.033112
1.8401	0.523316			
Total				0.546433 s^{-2}
Second peak: (2.465 - 3.025) MHz				
$\_B_0^E\_\_\_\_$	**$\triangle R_1/10^{-6}$**	**a+b**	**h**	**0.5*h(a+b)**
3.025	0.509654	1.655814	0.0873	0.072276
2.9377	1.14616	2.735918	0.0846	0.115729
2.8531	1.589758	3.252131	0.082	0.133337
2.7711	1.662373	3.102465	0.0809	0.125495
2.6902	1.440092	2.546282	0.077	0.098032
2.6132	1.10619	1.824598	0.0758	0.069152
2.5374	0.718408	1.290158	0.0722	0.046575
2.4652	0.571751			
Total				0.660596 s^{-2}
Overall				1.207029 s^{-2}

Therefore, for this 20% BSA sample, the areas under the quadrupole peaks at 2.1 MHz and 2.8 MHz were calculated to be 0.55 ± 0.01 s^{-2} and 0.66 ± 0.03 s^{-2} respectively, giving a total area of 1.21 ± 0.03 s^{-2}. Each calculated value has been reported with ±standard deviation.

The measurements were done at a constant temperature (of 25°C) to ensure that the samples did not suffer from denaturation or freezing. The NQR effect may not virtually occur in the liquid phase of samples, and so the samples for the experiments needed to be kept in gel form or fairly solid state to ensure that the NQR effect occurred and was accurately measured in the quadrupole peaks.

The "quadrupole dip" effect was largely studied in hydrated proteins and various biological samples in the early to mid-1980s. The first *in vivo* demonstration of the effect was carried out in living leeches by Kimmich., *et al*. [11]. Then in the 1990s, Lurie reported quadrupole dips *in vivo* in human muscle and brain using a whole-body sized field-cycling relaxometry and imaging system [2]. Subsequently, quadrupole dips have been measured in collagen fibers, calf lens [12] and multiple sclerosis plaques [5]. This study demonstrated an *in vitro* method of measuring quadrupole peaks (inverse of quadrupole dips) in laboratory-prepared protein samples by proposing a mathematical procedure for doing so.

In the dispersion profile, quadrupole dips are reported to occur at the specified field strengths of 16 mT, 49 mT and 65 mT, where cross-relaxation effects can be explored [1-4,11-13]. However, for sensitivity and signal homogeneity reasons, only field strengths of 49 mT and 65 mT were explored, corresponding to Larmor frequencies of 2.1 MHz and 2.8 MHz.

Sensitivity of the relaxometer to protein concentration changes

BSA concentration was positively correlated with quadrupole peak area, and from a regression fit of the data (Figure 11), the gradient gave a measure of the sensitivity of the FFC relaxometer to protein concentration measurement, which was 0.08 s^{-2}/% by weight.

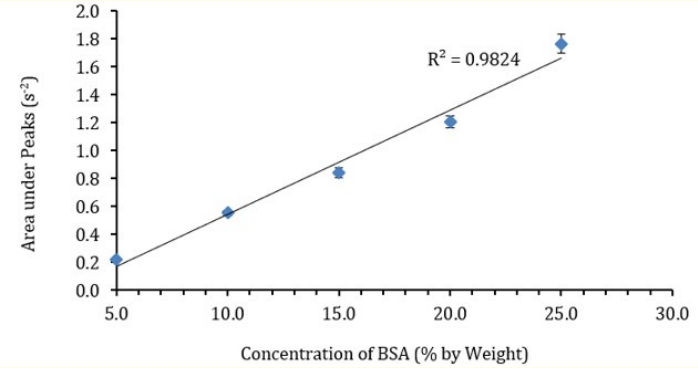

Figure 11: *Linear association between the total area under the quadrupole peaks and the protein concentrations of their respective BSA samples.*

Effect of agarose on relaxation dynamics of BSA

In a 1% BSA sample, varied concentrations of agarose were added and the observation was that increasing concentrations of agarose were associated with decreasing areas of the quadrupole peaks (Figure 12).

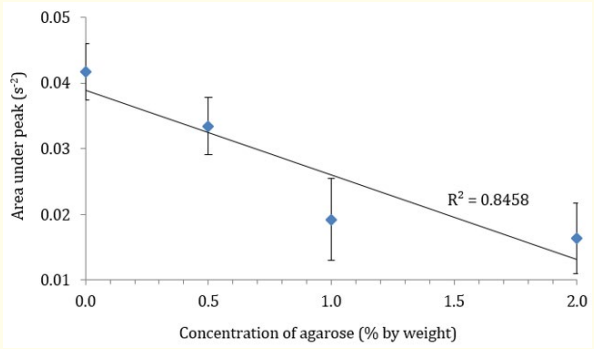

Figure 12: *Effect of varying concentrations of agarose on the size of the quadrupole peak at 2.8 MHz of 1% BSA. R^2 is the accuracy or 'goodness of the fit'.*

The results indicate that agarose is a relaxation-modifying agent, and that increasing the amount of agarose reduce the relaxivity of a fixed concentration of BSA and could, at a certain amount of agarose, null out the relaxation phenomena observed in BSA. This is possible because a relatively small concentration of BSA in a dense matrix of agarose is completely wound up tightly such that its protein protons almost no longer exhibit the quadrupolar resonance effect; hence the very low relaxation rates measured, due to prolonged T_1 relaxation times.

Effect of contrast agent on relaxation dynamics of BSA

$CuSO_4$ was used as the contrast agent in the experiments. Varying concentrations of $CuSO_4$ were added to a 10% BSA sample to observe the effect of the contrast agent on the relaxation dynamics of BSA. At a detection Larmor frequency of 2.5 MHz, it was observed that $CuSO_4$

enhanced (shortened) the background relaxation processes without affecting the size of the quadrupole peaks of the samples (Figure 13). The plots show how the quadrupole peaks compare with a 25% BSA sample without contrast. The results show that for the same BSA concentration, while agarose prolongs the T_1 relaxation time of BSA (as seen by the reduced peak areas), $CuSO_4$ shortens the quadrupole processes.

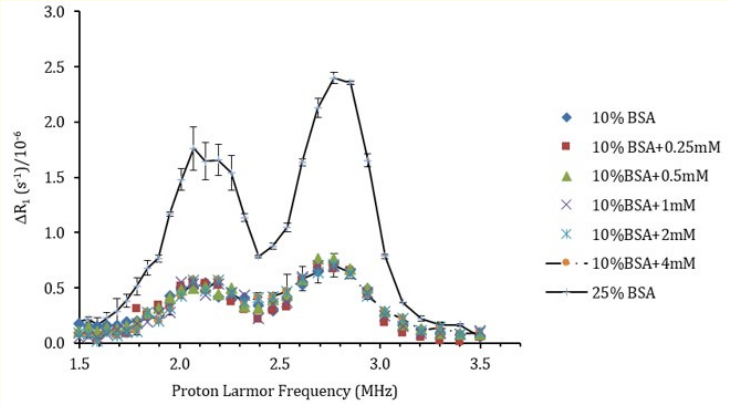

Figure 13: *Quadrupole peaks of varying concentrations of $CuSO_4$ in 10% BSA compared to the peak of 25% BSA without $CuSO_4$.*

Comparison of measured relaxivities between FC relaxometry and MRI

The relaxometry results have confirmed that the quadrupole peak size is proportional to the protein concentration of a given sample and that the size does not change in the presence of a contrast agent like $CuSO_4$. Based on this finding, relaxivities were measured from FC MR images of a composite phantom containing a BSA-$CuSO_4$ mixture (Figure 3). The image intensities measured were found to be proportional to the peak sizes of the protein gels, as expected [13].

Relaxivities measured on the composite phantom from MR imaging at 2.5 MHz were generally comparable to those from relaxometry in BSA samples without $CuSO_4$ (Table 2). However, samples with $CuSO_4$ showed considerable differences in their relaxivity results between relaxometry and MR imaging. Relaxivities estimated from MR imaging were higher than those estimated from relaxometry for samples with contrast.

Sample	Measured Relaxivity at 2.5 MHz	
	FC NMR Relaxometer	FC MRI System
5% BSA	1.55 ± 0.03	1.51
10% BSA	2.32 ± 0.02	3.17
15% BSA	4.45 ± 0.01	4.26
5% BSA + 18.7 mM $CuSO_4$	2.31 ± 1.27	4.69
10% BSA + 4.8 mM $CuSO_4$	2.90 ± 0.03	4.63
15% BSA + 3.7 mM $CuSO_4$	6.87 ± 0.06	5.88
4.3 mM $CuSO_4$	7.04 ± 0.09	8.62

Table 2: *Comparison between relaxometry and MR imaging relaxivity measurements at 2.5 MHz.*

The limitation of the MR imaging method was that measurements were not repeated to reduce the random error in each measurement. Secondly, inconsistencies in the selection of the regions of interest to estimate the relaxitivites could have also affected the accuracy of the measurements. Nonetheless, the samples without further modification to the BSA sample (with $CuSO_4$) indicated that the quadrupole peak calculation method was reliable.

Conclusion

By using a straightforward method to quantify quadrupole peaks emanating from cross-relaxation phenomena in proteins, changes in concentrations in protein samples were studied by relaxometry and the results indicated a linear association between protein concentration and size of the quadrupole peak, consistent with theoretical predictions. It was observed that the effect of a contrast agent on measured relaxivities may differ between NMR relaxometry and imaging.

Acknowledgements

Special thanks go to Prof. David J. Lurie and Dr. Gareth R. Davies of the University of Aberdeen for training the author on the use of the Stelar Fast Field Cycling Relaxometer, and granting him access to their laboratory to conduct the phantom studies.

Conflict of Interest

The author has no conflict of interest to declare.

Bibliography

1. Jiao X and Bryant RG. "Noninvasive measurement of protein concentration". *Magnetic Resonance in Medicine* 35.2 (1996): 159-161.
2. Lurie DJ. "Quadrupole-dips measured by whole-body field-cycling relaxometry and imaging". Proceedings of the International Society of Magnetic Resonance in Medicine 7th Meeting, Philadelphia, USA (1999): 653.
3. Rinck PA., *et al*. "Field-cycling relaxometry: medical applications". *Radiology* 168.3 (1988): 843-849.
4. Kimmich R and Esteban Anoardo E. "Field-cycling NMR relaxometry". *Progress in Nuclear Magnetic Resonance Spectroscopy* 44.3-4 (2004): 257-320.
5. Pine K. "Spatially Selective Field-Cycling NMR Relaxometry". MSc Thesis, Department of Bio-Medical Physics and Bio-Engineering, University of Aberdeen, Scotland, UK (2007).
6. Satheesh V., *et al*. "Technical Aspects of Fast Field Cycling NMR Relaxometry". Stelar s.r.l, Mede (PV) – 27035, Italy (2001).
7. Stelar Company Limited. "PC-NMR: Quick Start Manual". v.08.03. Mede (PV), Italy (2005).
8. Ferrante G and Sykora S. "Technical aspects of fast field cycling". *Advances in Inorganic Chemistry* 57 (2005): 405-470.
9. Lurie DJ., *et al*. "Design, construction and use of a large-sample field-cycled PEDRI imager". *Physics in Medicine and Biology* 43.7 (1998): 1877-1886.
10. Nusser W and Kimmich R. "Protein backbone fluctuations and NMR field-cycling relaxation spectroscopy". *Journal of Physical Chemistry* 94.15 (1990): 5637-5639.
11. Kimmich R., *et al*. "Interactions and fluctuations deduced from proton field-cycling relaxation spectroscopy of polypeptides, DNA, muscles, and algae". *Journal of Magnetic Resonance (1969)* 68.2 (1986): 263-282.

12. Beaulieu CF., *et al*. "Relaxometry of calf lens homogenates, including cross-relaxation by crystallin NH groups". *Magnetic Resonance in Medicine* 8.1 (1988): 45-57.

13. Davies GR., *et al*. "Protein Quantitation by Field-Cycling MRI". Workshop, 4th Conference on FC NMR Relaxometry, Torino, Italy (2005).

Volume 3 Issue 1 May 2024